Spectral improvements of recent GOCE GGMs through spatial selective filtering using wavelet-based multi-resolution approximation

A.C. Peidou, G.S. Vergos and D.A. Natsiopoulos

Department of Geodesy and Surveying, Aristotle University of Thessaloniki, Greece, vergos@topo.auth.gr

Introduction and Problem

The focus is on the improvement of the spectral behaviour of low resolution GOCE global geopotential models (GGMs) targeting the shortest resolvable wavelengths of their spectrum, i.e., at the limits of GOCE measurement waveband at d/o ~220-260.

At these spatial scales, GOCE signal is usually contaminated by noise. Therefore, spatial selective filtering using WL-based MRA is carried out at the first levels of WL decomposition.

The aim is a) to retrieve as much as possible of the useful GOCE signal, especially from the low-orbit GOCE data, and b) remove the inherent noise in the GOCE GGMs at the highest d/o of the GGM expansion.

The GGMs evaluated refer to the latest releases of GOCE GGMs, DIR-R5, TIM-R5 and GOCO03s, while EGM2008 is used as reference.

Also an investigation of the coherence and the correlation between the GOCE GGMs and land topography is carried out, the latter being represented the SRTM DTM.

Methodology- Synthesis

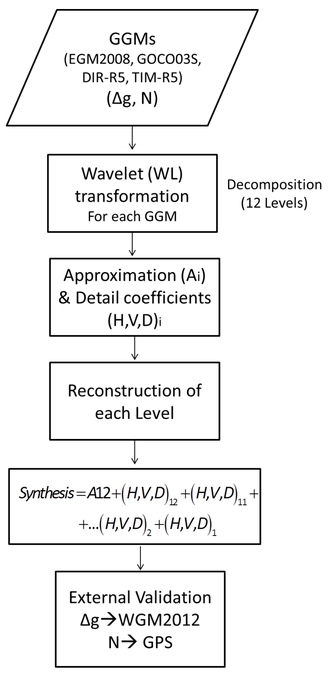

Figure 1: Methodology for WL MRA Synthesis process

Table 1: Statistics of the gravity anomaly differences between WGM2012 and GGMs before and after the WL MRA synthesis. Units: [mGal]

	min	max	mean	std
EGM08	-49.66	128.5	0.31	±3.24
GOCO03s	-204.97	272.23	0.11	±22.49
GOCO03s (L_5,L_6, L_7)	-89.09	129.87	0.32	±9.38
GOCO03s (L_6, L_7)	-51.19	123.95	0.31	±3.52
TIM-R5	-196.9	272.7	0.11	±19.34
TIM-R5 (L_5,L_6, L_7)	-59.78	129.77	0.49	±7.66
TIM-R5 (L_6, L_7)	-40.53	124.22	0.43	±3.37
DIR-R5	-203.66	270.65	0.11	±19.10
DIR-R5 (L_5,L_6, L_7)	-65.17	129.42	0.54	±7.38
DIR-R5 (L_6, L_7)	-41.02	125.5	0.41	±3.35

Table 2: Statistics of geoid height differences between GPS and the GGMs before and after the WL MRA synthesis. Units: [m]

	min	max	mean	std
EGM08	-0.85	0.104	-0.37	±0.134
GOCO03s	-1.74	1.11	-0.36	±0.464
GOCO03s (L_5,L_6, L_7)	-1.08	0.453	-0.39	±0.259
GOCO03s (L_6, L_7)	-0.86	0.093	-0.38	±0.124
TIM-R5	-1.57	1.123	-0.39	±0.469
TIM-R5 (L_5,L_6, L_7)	-1.14	0.408	-0.39	±0.242
TIM-R5 (L_6, L_7)	-0.83	0.047	-0.38	±0.121
DIR-R5	-1.53	1.122	-0.39	±0.454
DIR-R5 (L_5,L_6, L_7)	-1.03	0.388	-0.39	±0.217
DIR-R5 (L_6, L_7)	-0.81	0.032	-0.38	±0.118

Table 3: Standard deviation of ΔG differences between WGM2012 and the GGMs before and after the WL MRA synthesis and filtering. Units: [mGal]

	Initial	Synthesis (L5,L6,L7)	Spatial (Gaussian)	Selective filtering
TIM-R5	±19.34	±7.66	±5.73	±4.92
DIR-R5	±19.10	±7.38	±5.63	±4.93
GOCO03s	±22.49	±9.38	±6.48	±5.05

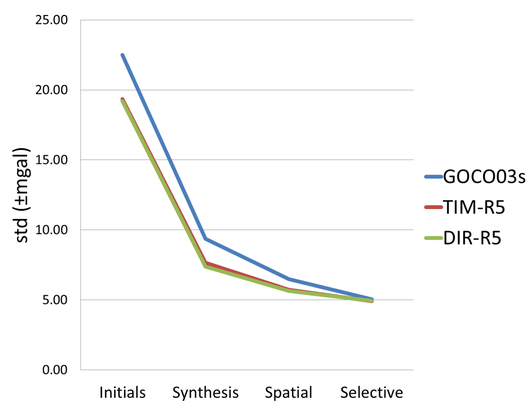

Figure 6: Standard deviations between WGM2012 gravity anomalies (Δg) and hybrid GGMs.

Table 4: Standard deviation of geoid height (N) differences between GPS and the GGMs before and after the WL MRA synthesis and filtering. Units: [m]

	Initial	Synthesis (L5,L6,L7)	Spatial (Gaussian)	Selective filtering
TIM-R5	±0.469	±0.242	±0.213	±0.157
DIR-R5	±0.454	±0.217	±0.187	±0.149
GOCO03s	±0.464	±0.259	±0.176	±0.169

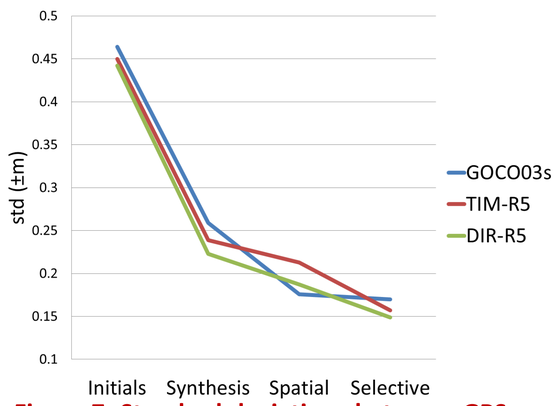

Figure 7: Standard deviations between GPS geoid heights and hybrid GGMs.

Table 5: Statistics of the gravity anomaly differences between WGM2012 and GGMs after filtering. Units: [mGal]

Filtering	min	max	mean	std
TIM-R5-f (L_5,L_6, L_7)-Gauss	-51.01	130.51	1.09	±5.73
TIM-R5-f (L_5,L_6, L_7)-Boxcar	-53.43	134.46	1.35	±6.19
TIM-R5-f(L_5,L_6, L_7)-Selective	-66.47	127.58	0.29	±4.92
DIR-R5-f (L_5,L_6, L_7)-Gauss	-53.83	129.66	1.09	±5.63
DIR-R5-f (L_5,L_6, L_7)-Boxcar	-55.7	132.9	1.35	±6.14
DIR-R5-f(L_5,L_6, L_7)-Selective	-64.65	126.63	0.30	±4.93
GOCO03s-f (L_5,L_6, L_7)-Gauss	-72.77	127.91	0.31	±6.48
GOCO03s-f (L_5,L_6, L_7)-Boxcar	-74.65	130.64	0.32	±6.94
GOCO03s-f(L_5,L_6, L_7)-Selective	-63.44	126.76	-0.31	±5.05

Table 6: Statistics of the geoid height differences between GPS and GGMs after filtering. Units: [m]

Filtering	min	max	mean	std
TIM-R5-f (L_5,L_6, L_7)-Gauss	-1.011	0.314	-0.373	±0.213
TIM-R5-f (L_5,L_6, L_7)-Boxcar	-0.927	0.279	-0.377	±0.190
TIM-R5-f(L_5,L_6, L_7)-Selective	-0.929	0.181	-0.387	±0.157
DIR-R5-f (L_5,L_6, L_7)-Gauss	-0.925	0.279	-0.378	±0.187
DIR-R5-f (L_5,L_6, L_7)-Boxcar	-1.027	0.316	-0.373	±0.212
DIR-R5-f(L_5,L_6, L_7)-Selective	-0.885	0.164	-0.385	±0.149
GOCO03s-f (L_5,L_6, L_7)-Gauss	-0.870	0.206	-0.377	±0.176
GOCO03s-f (L_5,L_6, L_7)-Boxcar	-0.898	0.244	-0.373	±0.192
GOCO03s-f(L_5,L_6, L_7)-Selective	-0.892	0.183	-0.380	±0.169

Spatial and Selecting Filtering

Two types of isotropic filters, i.e. a boxcar and a Gaussian one have been tested in order to investigate whether they improve the results for the synthesized GGMs.

Spatial low pass filters applied to decomposition Level 5. The 120 km cut-off frequency was the one providing the most rigorous results.

Selective filtering was implemented by removing noisy frequencies from L5. To detect the noisy frequencies RDA PSDs of each signal was calculated. By comparing RPA of GOCE/GRACE GGMs with EGM08 RPA the noisy frequencies were detected. A digital filter that follows the trend of the difference between RPAs was designed and implemented.

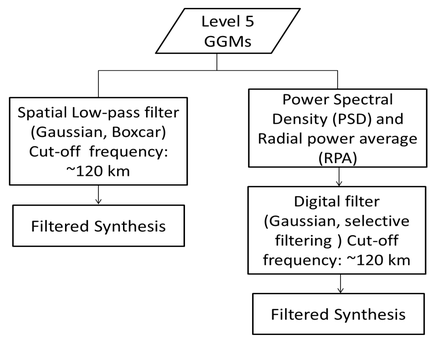

Figure 2: Methodology for spatial and selective filtering

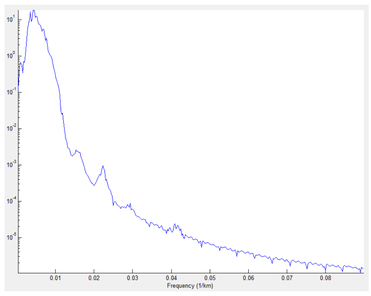

Figure 3: RPA ΔG Level 5 EGM08

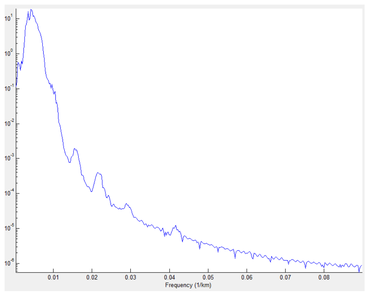

Figure 4: RPA ΔG Level 5 DIR-R5

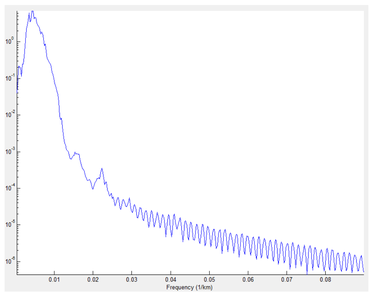

Figure 5: RPA ΔG Level 5 DIR-R5 (Selective filtering)

Table 7: Correlation between Topography (SRTM derived) and GGM-derived gravity anomalies (%) (Red color indicates correlation after selective filtering implementation)

	EGM2008	GOCO03s	TIM-R5	DIR-R5
L_1	22.1	49.6	48.0	48.6
L_2	78.2	20.5	19.3	20.0
L_3	84.0	6.1	3.4	2.9
L_4	80.1	34.2	42.2	42.6
L_5	***67.0***	***61.0***	***62.5***	***63.4***
L5	**67.0**	**67.5**	**67.3**	**67.3**
L_6	64.3	64.2	64.3	64.3
L_7	57.2	57.5	57.5	57.6
L_8	65.3	66.1	65.3	65.4
L_9	48.4	45.4	45.5	44.6
L_{10}	15.9	18.7	20.6	20.0
L_{11}	67.6	64.7	73.4	73.2
L_{12}	56.2	20.9	26.0	21.5

EGM08 shows higher correlation for the first 5 levels compared to GOCE/GRACE GGMs. However, after selective filtering implementation the correlation of these GGMS is significantly improved by ~5%, showing better spectral behavior than EGM08. Coherency between Topography and EGM08 gravity anomalies indicates the high power transfer between the signals, especially in wavebands ~80-120 km (Figure 8). GOCE/GRACE GGMs are satellite-based models and hence coherency is lower. Figure 9 reveals a higher spectral coherency, between topography and GGMs after implementing selective filtering on Level 5.

GGMs and Topography Correlation and Coherence

The spectral coherence examines the relation between two signals. It is commonly used to estimate the power transfer between input and output of a linear system.

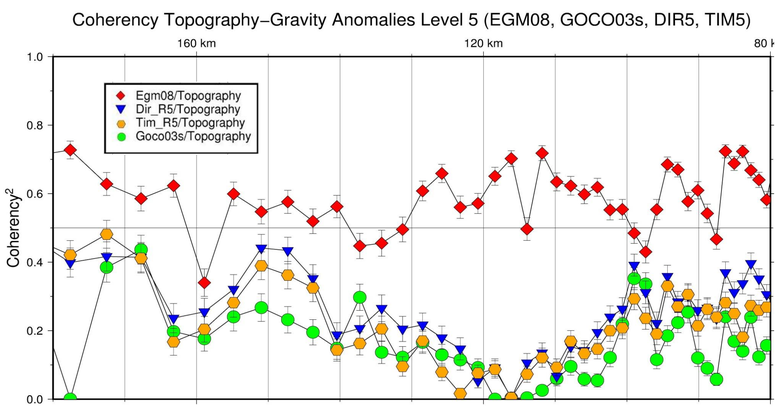

Figure 8: Topography (SRTM derived) and GGMs' Gravity anomalies Coherency Level 5

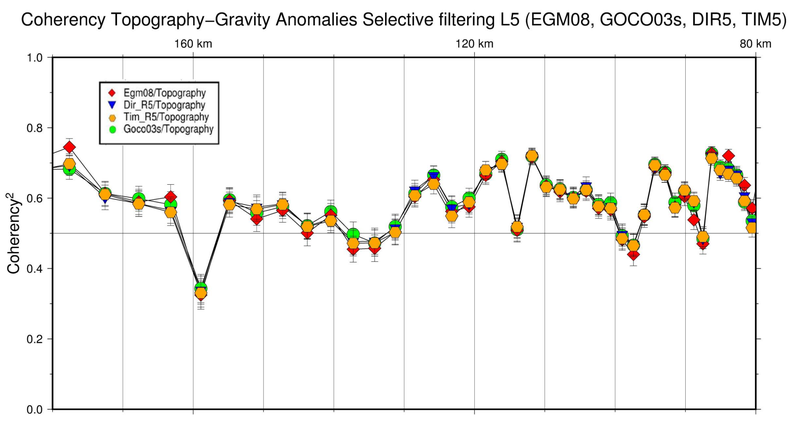

Figure 9: Topography (SRTM derived) and GGMs' Gravity anomalies Coherency after implementing selective filtering on Level 5

Conclusions

A detailed validation of GOCE/GRACE GGMs conducted through WL MPA. Synthesis hybrid GGMs improved gravity anomalies by ±15mgal and geoid heights by ±20cm. Spatial low-pass filters implemented on L5 further hybrid GGMs by ±3mgal and ±8cm respectively. Finally, selective filtering technique, removed noisy frequencies and increased the SNR by improving ±5mgal (Δg) and ±10cm (N) synthesis hybrid GGMs. The wavebands 44~704km are high correlated for all the GGMs, while EGM08 displays a higher cross-correlation compared to the GOCE/GRACE GGMs. Coherency reveals a high power transfer between topography and EGM08, while GOCE/GRACE GGMs show considerably low coherency in the waveband 90~130 km. The advent brought by selective filtering was further assessed by the improvement of coherency by ~0.2 in the L5 waveband.

IUGG 2015 General Assembly, Session G02 "Static Gravity Field Models and Observations", G02p-458
June 22-July 2, 2015, Prague, Czech Republic